Time-Series Spectroscopy of Pulsating Stars

Ivan Karim Baldry

A thesis
submitted for the degree of
Doctor of Philosophy
at the
University of Sydney

25th March 1999

Declaration of Originality

This thesis contains no material which has been presented for a degree at this or any other university and, to the best of my knowledge and belief, contains no copy or paraphrase of work published by another person, except where duly acknowledged in the text.

Note that Chapters 4–7 are written in the third person, because they are based on MNRAS papers produced in collaboration with other astronomers (Baldry et al. 1997, 1998b, 1998c, 1999). Nevertheless, they are a valid part of my thesis because the majority of the work can be credited as my own. The division of work is explained at the beginning of each of these chapters.

Ivan K. Baldry

Summary

Time-series spectroscopy of pulsating stars

The study of pulsating stars adds an extra dimension to stellar astrophysics. In addition to intensity measurements of a stellar spectrum, pulsational variations of a spectrum can be studied. These variations can be described by frequencies, amplitudes and phases of oscillations in various quantities derived from the spectrum. The frequencies of acoustic oscillations depend on the sound speed throughout the star, while the amplitudes depend on the excitation and damping processes. For spectroscopy, the observable quantities include Doppler shifts, equivalent widths and profile measurements of spectral lines. The variations of these observables are mainly related to velocity and temperature changes in the atmosphere of the star. In this thesis, spectral variations of the Cepheid ℓ Car and two rapidly oscillating Ap stars (roAp stars), α Cir and HR 3831, are analysed.

CCD non-linearity

For the roAp star spectra, the signal-to-noise ratios were sufficiently high that it was worth making a non-linearity correction to the CCD data. Non-linearity measurements of two CCDs at Mt. Stromlo Observatory are presented.

A ratio method is developed which involves measuring the intensity ratio between two regions on the CCD (after bias correction), using a flat-field lamp for illumination. In order to determine the non-linearity, the ratio is measured for exposures of varying length. For a linear CCD, the measured ratio should be the same for all exposures. This method can provide an accurate non-linearity curve because it is unaffected by uncertainties in the exposure time, and it is less affected by changes in the lamp's flux than for other methods.

ℓ Carinae

ℓ Car is a Cepheid with a pulsation period of 35.5 days. The variation of the Hα profile is presented, using 33 high-resolution echelle spectra obtained between February 1994 and April 1995.

A weak Hα emission feature is present at nearly all phases, which is unusual for classical Cepheids. This emission appears both redward and blueward of the absorption feature at different phases. The origin of the emission feature may be a shock front or may be the upper atmosphere of the star.

α Circini

α Cir is an roAp star with one dominant pulsation period of around 6.8 minutes. Over 6000 spectra of the wavelength region 6000–7000Å were obtained, from dual-site observations with medium-dispersion spectrographs during two weeks in May 1996. Several different measurements are presented, including velocities of different spectral lines and line-profile measurements of the Hα line.

The velocity amplitude and phase of the principal pulsation mode vary significantly, depending on which line is being measured. The amplitude is observed to be as high as $1000\,\mathrm{m\,s^{-1}}$ in some wavelength bands, despite a previous upper limit of $36\,\mathrm{m\,s^{-1}}$. Furthermore, some lines are apparently pulsating in anti-phase with others. This may indicate a high-overtone standing wave with a velocity node in the atmosphere of the star.

Additionally, the bisector-velocity amplitude and phase vary significantly, depending on the height in the Hα line, including a phase reversal between the core and the wings of the line. This supports the theory of a radial pulsational node in the atmosphere of the star. Blending with metal lines partially affects the Hα bisector results but probably not enough to explain the phase reversal.

Changes in the equivalent-width of the line during the pulsation, and the oscillatory signal as a function of wavelength across the Hα region, are also presented.

HR 3831 (IM Velorum)

HR 3831 is an roAp star with a pulsation period of around 11.7 minutes. 1400 medium-resolution spectra of the wavelength region 6100–7100Å were obtained, during one week in March 1997. Similar measurements to those made on α Cir are presented.

The Hα velocity amplitude of HR 3831 is modulated with rotation phase. Such a modulation was predicted by the oblique pulsator model, and rules out the spotted pulsator model. However, further analysis of the Hα line and other spectral lines suggests that there are rotational modulations which cannot easily be explained using the oblique pulsator model.

The variation of the Hα bisector shows a very similar pattern to that observed in α Cir. This argues against the radial node interpretation since HR 3831 has a longer period and therefore the pulsation is expected to have a longer vertical wavelength in the atmosphere of the star, unless the structure of the atmosphere is somewhat different between the two stars. Alternatively, the bisector variation is a signature of the degree ℓ of the mode and not the overtone value n.

High-resolution studies of the metal lines in roAp stars are needed to understand fully the form of the pulsation in the atmosphere.

Acknowledgements

First and foremost, I would like to thank my parents, Mum and Dad, Liz and Allan, for always supporting me in my education and my interest in astronomy.

Before coming to Sydney, I studied at King's College in Cambridge for four years and worked at the Isaac Newton Group on La Palma over two summers. I am grateful to all who helped me at these institutions, in particular, to those who provided the references for my PhD application, Chris Gilligan at King's and Mike Breare at the ING. Oh and how could I forget to mention Ju, Stu, Mark, Gez and Sam for plenty of moral support.

During my PhD, I was part of the Chatterton Astronomy Department in the School of Physics at the University of Sydney. I am very grateful to Tim Bedding for being a jolly good supervisor and to John Davis for giving me the opportunity to do a PhD. I would also like to thank Andrew Booth, Siou-Gek Chew, Sonia Cianci, David Dawes, Andrew Jacob, Andreas Kelz, Alberto Mendez, Anna Moore, Melinda Taylor, Erik Thorvaldson and the rest of the Astronomy Department. Other people in the School of Physics have also been helpful throughout the course of my thesis: Lawrence Cram, Gene Davidson, Bryan Gaensler, Tanya Hill, Alex Merchant and many others.

The observations for my thesis were obtained at Mt. Stromlo Observatory. I am very grateful to Mike Bessell and other staff at MSO for their help and advice.

During 1996, I spent three months at the Institut for Physik og Astronomi, University of Aarhus. This really kick-started my PhD, working closely with Jörgen Christensen-Dalsgaard, Sören Frandsen, Hans Kjeldsen and Michael Viskum. Hans has effectively been my co-supervisor. After these three months, in October 1996, I went to the conference in Nice on 'Sounding Solar and Stellar Interiors'. Here, I met some of the experts on roAp and Ap stars. In particular, I would like to thank Jaymie Matthews, Thebe Medupe, Don Kurtz and Friedrich Kupka for many discussions.

That covers nearly everyone, but there are some other people that I would like to thank: my relatives in Perth for accommodation and support when I arrived in Oz in 1995; Wendy Page and her family for the same when I arrived in Sydney; Felicity Baldry, Michael Barnes, Tracy Bryan, Andrew Harrison, Stefan Keller, Glenn Mitchell, Eileen O'Hely, Stefanie Sander, Eliza Skinner, Kelly Tsoi and other friends in Sydney; bushwalking, climbing and squash club members for recreation.

Thanks to all those co-authors who contributed to producing my first publication, a song about the Winter ASA (Baldry et al. 1996). Admittedly, I wrote none of the lines and only gave moral support but, because of alphabetical order, I get to be first author. I mention it here because this is the only chance that I'll get to cite it.

Financial assistance was obtained from the Australian Postgraduate Award, Australian Research Council and the Danish Natural Science Research Council.

Contents

List of Figures

List of Tables

Chapter 1

Pulsating stars

1.1 Introduction

Pulsating stars: vibrating, oscillating, resonating — or, for a more official definition, "pulsating variables are stars showing periodic expansion and contraction of their surface layers" (General Catalogue of Variable Stars, GCVS). They also change temperature and luminosity in a periodic or quasi-periodic way. This is not an unusual phenomenon amongst stars, and known types of pulsating stars cover a large range of stellar masses and ages. It is possible that all stars are oscillating or pulsating to some extent but that most have amplitudes that are too low to detect with present technology. For instance, the Sun has oscillations with periods around five minutes and with very small amplitudes, which are only detectable because of our proximity. However, when astronomers use the term *pulsating stars*, they are usually referring to stars where the oscillations are driven by a feedback mechanism within the star[1]. In these stars, one or more oscillation modes are intrinsically unstable (self-excited), and the star is observed as being singly- or multi-periodic. Known pulsation periods range from about one minute in some white dwarfs up to about five years in some supergiants.

The observational challenges of studying pulsating stars involve answering the question: in what way is the spectrum or radiation from a star changing? In particular, what are the frequencies and amplitudes of the vibrations, and how are the amplitudes and phases of different measurements (e.g., magnitudes, Doppler shifts) related to each other? The theoretical challenges involve answering the question: how and why is a star pulsating? In particular, what are the temperature, velocity and density changes during the pulsation, as a function of position in the star, and what causes the star to oscillate (pulsation mechanism)?

Apart from being interesting astrophysical objects in their own right, pulsating stars are of importance to other fields, for example: (i) stellar atmospheres and interiors, (ii) stellar evolution, (iii) the distance scale. The next three paragraphs briefly describe some aspects of these cases.

In the first case, the frequencies of acoustic oscillations are related to the sound-speeds within a star, and measuring these frequencies provides an excellent test of stellar models. For this purpose, it is important to determine the type of mode for each observed frequency. Modelling atmospheres and interiors is closely related to modelling pulsations, since knowledge of the temperature and density structure within a star is essential to understanding causes and effects of the pulsation.

In the second case, evolution, oscillation frequencies can be measured more accurately than any other stellar property (radius, luminosity, etc.), and therefore it is possible to: (a) accurately define evolutionary states, ages and masses within a class of pulsating stars, and (b) measure changes in some stars over time periods of years. For example, a few pulsating white dwarfs have been observed to change very slightly in period over several years (Sullivan 1998). This is possibly due to changes in the oscillation frequencies of a white dwarf as it cools over an evolutionary time scale.

[1] Under this definition, the Sun and other stars, with similar low-amplitude oscillations, are not included since their oscillations are excited randomly by convection.

In the third case, the distance scale, many classes of pulsating stars have a relationship between their period and luminosity. Generally the bigger and brighter a star is, within a class, the longer the pulsation period. The best known case is for classical Cepheids, where there is a close period-luminosity relationship. Therefore, in order to estimate a Cepheid's absolute luminosity, it is only necessary to measure its period. Then, by measuring the star's apparent luminosity, an estimate of the distance to the star can be obtained. Using the Hubble telescope, the distance can be obtained to Cepheids up to 20 Megaparsecs away, which provides a major step in the extra-galactic distance scale.

In the rest of this chapter, I give a broad picture of pulsating stars, in terms of different types of oscillation modes (asteroseismology) and different types of stars. The following chapters (2–3) give some technical details of observing, data reduction and CCD non-linearity.

In the chapters presenting the scientific results of this thesis (4–7), I quantitatively analyse the spectral changes in three pulsating stars: the long-period Cepheid ℓ Carinae and two rapidly oscillating Ap stars (roAp stars), α Circini and IM Velorum (better known as HR 3831), mainly looking at changes around the Balmer line Hα. Qualitative analysis is given for the form of the pulsation in the atmospheres of the stars.

1.2 Asteroseismology

The study of the oscillation modes in multi-periodic stars is called asteroseismology. In this section, the classification of the different types of modes is explained.

All stars have eigenmodes with associated frequencies at which they can vibrate (analogous to the modes on the membrane of a drum). The surface variation of these modes can be closely described using spherical harmonic functions, $Y_{\ell m}$, which are well known from the quantum mechanical description of the hydrogen atom. Modes with $\ell = 0$ are radial (because the motion is entirely in the radial direction), and with $\ell \geq 1$ are non-radial. The frequencies of modes with the same 'angular degree' ℓ can be split by rotation into $2\ell + 1$ different frequencies, with the 'azimuthal order' m taking values between $-\ell$ and $+\ell$. The ℓ value is equal to the number of nodal lines on the surface, with $|m|$ indicating how many nodal lines pass through the poles of some axis[2] of physical symmetry in the star. Additionally, there is a quantum number n which is the overtone value of the pulsation. The 'radial order' n is equal to the number of nodes on a radial line between the surface and the centre of the star (called *radial nodes* in this thesis).

The eigenmodes of a star are often divided into p, f and g modes. For p-modes, the restoring force is gas and radiation pressure. These are basically standing sound waves within the star, for which the frequency of the oscillations increases with increasing overtone. The g-modes vibrate at lower frequencies and the restoring forces are gravity and buoyancy force. These have mostly horizontal motions and the frequency decreases with increasing overtone. There are only non-radial g-modes. The intermediate f-modes or fundamentals have no nodes in the radial direction ($n = 0$), and are generally considered

[2]Usually the rotation axis, but in the case of roAp stars the magnetic axis is the relevant axis in the oblique pulsator model.

to be the lowest frequency p-modes. The $\ell = n = 0$ mode is the fundamental radial mode seen, for example, in classical Cepheids. Note that the fundamental dipole mode ($\ell = 1$, $n = 0$) is forbidden because it violates conservation of momentum.

The roAp stars pulsate in high-overtone p-modes. For these mode frequencies ($n \gg \ell$), there is a useful 'asymptotic theory' approximation to the frequencies (Christensen-Dalsgaard 1988; Brown & Gilliland 1994):

$$\nu_{n,\ell} \simeq \Delta\nu_0(n + \ell/2 + \epsilon) - \ell(\ell+1)D_0 + ..., \tag{1.1}$$

where $\Delta\nu_0$, ϵ and D_0 are constants which depend on the structure of the star. Modes with the same degree ℓ but different n are separated in frequency by multiples of $\Delta\nu_0$, which is called the 'large separation'. This parameter is related to the sound travel time through the star and, using the virial theorem, it can be shown that it is simply related to the mean density of the star (Brown & Gilliland 1994):

$$\nu_{n,\ell} - \nu_{n-1,l} \simeq \Delta\nu_0 \approx 135\sqrt{\frac{M/M_\odot}{(R/R_\odot)^3}}\,\mu\mathrm{Hz}. \tag{1.2}$$

This equation is expected to hold for stars of various masses along the main-sequence. There is also a relationship between the frequencies of modes differing by two in degree, which can be written as:

$$\delta\nu_{n\ell} = \nu_{n,\ell} - \nu_{n-1,\ell+2} \approx (4\ell+6)D_0. \tag{1.3}$$

$\delta\nu$ is called the 'small separation' and is about a factor of ten smaller than the large separation (Christensen-Dalsgaard 1988), between modes of $\ell = 0$ and 2. This parameter is related to the sound-speed in the core and is therefore sensitive to the age of the star because, as hydrogen burns to form helium, the sound-speed in the core changes.

Modes with $\ell \leq 3$ are of the most significance to observational asteroseismology, since modes with higher ℓ values are extremely hard to detect in integrated light or velocity. This is because observed light variations are an integral over the surface of the star, and high-degree modes have many phase changes across a stellar hemisphere.

Considering high-overtone p-modes obeying the asymptotic theory: (a) if $\ell = 0$ and 1 modes are observed in star, then the oscillation spectrum[3] would consist of peaks at roughly equally spaced frequencies separated by $\Delta\nu_0/2$, (b) if $\ell = 0$–3 modes are observed, then the oscillation spectrum would be similar except doublets would be present in place of single peaks. The oscillation spectrum can be further complicated by rotational splitting.

Many roAp stars have modes that are separated in frequency by multiples of $\Delta\nu_0/2$, because they pulsate in high-overtones with possibly $\ell = 1$ and 2 modes observed. A good example is the roAp star HR 1217 which has five equally-spaced modes, of which, four are rotationally split into triplets (Kurtz et al. 1989). α Cir has five known modes

[3]An 'oscillation spectrum' is a Fourier transform of the light or spectral variations in a star. It can be shown as an 'amplitude spectrum' or a 'power spectrum' (amplitude or amplitude squared versus frequency, respectively).

in the range 2250–2600 μHz, with one showing rotational splitting. Kurtz et al. (1994b) inferred a large separation of 50 μHz from the fact that the frequency spacings between the modes were all nearly integer multiples of 25 μHz.

1.3 Classification

There are many types of pulsating star and more types being discovered every decade. In this section, I briefly describe some of the classifications which are divided into three general groups in terms of their position in the H-R diagram: (i) stars evolved significantly above the zero-age main-sequence (ZAMS), which all pulsate radially in fundamental or low-overtone p-modes; (ii) stars on or near the main-sequence; (iii) stars evolved below the ZAMS.

Figure 1.1 shows the locations of some of these pulsating stars in the H-R diagram diagram (provided by J. Christensen-Dalsgaard). The shading is related to the excitation and the type of modes; (a) horizontal shading indicates stochastically excited p-modes, (b) NW-SE shading (like Cepheids) indicates self-excited (predominately) p-modes, (c) SW-NE shading (like DAV) indicates self-excited g-modes.

The zero-age main-sequence is represented by a single *dashed-line*, while the Cepheid-instability strip is confined by *parallel dashed-lines*. The evolution of various mass stars from the main-sequence to the giant and supergiant phases are represented by *solid lines* (initial masses of 1, 2, 3, 4, 7, 12 and 20 solar masses). After the red-giant phase, some low-mass stars (initial $M \lesssim 2M_{\odot}$) go through a stable phase of evolution where the star becomes condensed and blue. These stars form a 'horizontal branch' in the H-R diagram represented by the *dash-and-dotted line*. In the final stages of evolution, intermediate- and low-mass stars (initial $M \lesssim 7M_{\odot}$) shed most of their outer layers leaving a core, which firstly contracts and heats-up forming a pre-white dwarf (surrounded by a planetary nebula), before cooling to become a white dwarf. These stages are represented by the *dotted line*[4].

For the stars analysed in this thesis, their positions ($\log T_{\rm eff}, \log L/L_{\odot}$) in the H-R diagram are about: (3.7,4.2) for the classical Cepheid ℓ Car (mean position); (3.90,1.06) for the roAp star α Cir; and (3.90,1.13) for the roAp star HR 3831.

Several references were used to obtain the information on the pulsating stars described below. The general references were: (a) for classifications: Feast (1992), Becker (1998) and the GCVS (Kholopov et al. 1998); (b) for details on each class of pulsating stars: recent conference proceedings (Stobie & Whitelock 1995; Provost & Schmider 1997; Bradley & Guzik 1998; Deubner et al. 1998), review articles (Brown & Gilliland 1994; Gautschy & Saio 1995, 1996) and an astronomy encyclopedia (Marin 1992); (c) for periods of the white-dwarf and pre-white-dwarf stars: data tables by Bradley (1995).

Note that in these descriptions: (a) low-overtone modes have n less than about 5, and high-overtone modes have n greater than about 20; (b) all amplitudes quoted are full-range amplitudes.

[4]No star is actually seen crossing from the giant region to the planetary nebulae nuclei (PNN) region. When a giant star expands enough, the core shows through — there are no intermediate stages.

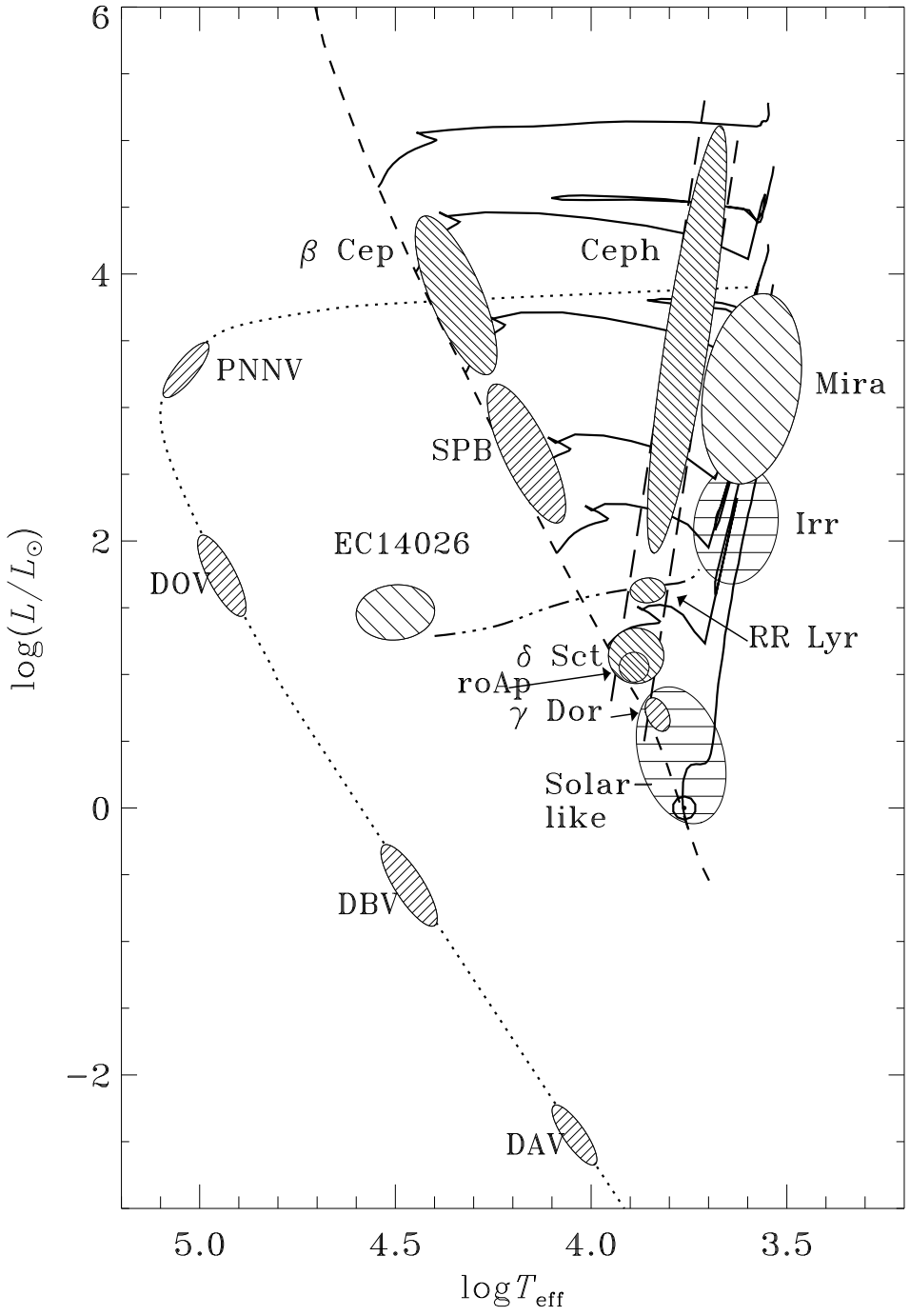

Figure 1.1 Schematic H-R diagram showing the location of several classes of pulsating stars, provided courtesy of Jørgen Christensen-Dalsgaard (private communication). The shading is related to the excitation and the type of modes, while the lines represent various evolutionary tracks and states. See text for details.

Group I: above the main-sequence, radial p-modes

- Miras — periods: 80–1000 days
  — Miras are pulsating red-giant stars with large amplitudes. They are 10 to 4000 times brighter in visible light at maximum than at minimum (amplitude 2.5–9 mag in V), and show considerable irregularity in the amplitude and shape of the light curve. There is some dispute as to whether they pulsate primarily in their fundamental or first overtone (Wood 1995), and there is evidence that some Miras switch between different modes on time scales of decades (Bedding et al. 1998).
- Irregular (Irr) and semi-regular (SR) variables — periods: 20–2000 days
  — These are similar to Miras but with poorly defined periods and generally lower amplitudes (< 2.5 mag in V). The term long-period variable (LPV) is often used to cover all pulsating red giants and supergiants (Whitelock 1990).
- Cepheids (δ Cephei stars) — periods: 1–70 days
  — Cepheids are pulsating yellow supergiants with luminosities 500 to 30 000 times larger than that of the Sun, but with similar effective temperatures. The light amplitudes are typically between 0.5 and 2 magnitudes. The classical Cepheids pulsate in the fundamental radial mode and have a close period-luminosity relationship, which has given them an important role in determining the distance to nearby galaxies. Other Cepheids pulsate in their first overtone, or simultaneously in their fundamental and first overtone (beat Cepheids).
- Type II Cepheids (RV Tau stars, W Vir stars, BL Her stars) — periods: 0.8–150 days
  — These are pulsating variables of the old spherical component (halo) of the galaxy. They are similar to classical Cepheids and they also obey a period-luminosity relationship. For a similar period, the Type II Cepheids are fainter by about 1–2 mag. They are often divided into three types based on their period; RV Tau ($P > 30$ d), W Vir (intermediate period) and BL Her ($P < 8$ d) stars.
- R Coronae Borealis (RCB) stars [5] — periods: 30–100 days
  — RCB stars are hydrogen-poor and carbon-rich giants. Many have been observed to have Cepheid-like pulsations.
- RR Lyrae stars — periods: 0.2–0.9 days (5–22 hours)
  — RR Lyr stars are old low-mass ($M \sim 0.7 M_\odot$) giant stars, with A to F spectral type. They pulsate radially in their fundamental or first overtone modes, with amplitudes between 0.2 and 2 mag in V. In the H-R diagram, they are located just below the Cepheids in the 'Cepheid instability strip'.

Group II: on or near the main-sequence

- β Cephei stars (β Canis Majoris stars) — periods: 0.1–0.3 days (2.5–7 hours)
  — These are pulsating early-type-B stars, which are multi-periodic with amplitudes less than 0.3 mag in V. Pulsational variability is common amongst O and B stars, of

[5] In the GCVS, classified under *eruptive variable stars*.

which, the β Cep stars were the first to be discovered. In the β Cep domain, radial and non-radial, fundamental and low-overtone p- and g-modes are expected to be unstable (Moskalik 1995).

- Slowly pulsating B (SPB) stars (53 Per stars) — periods: 0.5–4 days (12–96 hours) — SPB stars are mid-type-B to late-type-B stars, with variability on time-scales of about a day. The multi-periodic nature of these variations means that they can only be understood in terms of pulsations (Waelkens 1996). In particular, they must pulsate in non-radial g-modes, because their periods are significantly longer than the expected periods for fundamental modes.
- δ Scuti stars — periods: 0.5–8 hours
  — δ Sct stars are mostly main-sequence and sub-giant stars, of spectral class A and early-type-F. They pulsate in many modes, with amplitudes less than 0.8 mag. As with the β Cep stars, radial and non-radial, p- and g-modes are excited. The high-amplitude (> 0.1 mag) δ Scuti stars comprise less than 10% of the class, and are usually sub-giant to giant stars. On the main-sequence, they generally have small amplitudes of around 0.02 mag (Breger 1979).
- Rapidly oscillating Ap (roAp) stars [6] — periods: 0.08–0.25 hours (5–15 minutes)
  — roAp stars are a sub-group of the chemically peculiar magnetic stars that pulsate in high-overtone p-modes (pulsating CP2 stars), with amplitudes less than 0.02 mag. They occupy approximately the same region of the H-R diagram as the main-sequence δ Sct stars, but pulsate in much higher overtones. This is probably due to their strong magnetic fields.
- γ Doradus stars — periods: 0.5–3 days (12–72 hours)
  — γ Dor stars are main-sequence early-type-F stars. For similar reasons to the SPB stars, their variability has been associated with non-radial g-modes. They are a new class of pulsating stars, discovered this decade (Balona et al. 1994).
- Solar-like oscillators — periods: 0.08–0.33 hours (5–20 minutes)
  — These stars, late-type-F to G, are expected to oscillate in a similar way to the Sun, in which, many p-modes are excited by stochastic convection across a range of periods with amplitudes below 5×10^{-5} mag. The highest amplitude modes have periods of about 5 minutes in the Sun, and are expected to have periods of around 20 minutes in the sub-giants. No solar-like oscillations have been confirmed in a star other than the Sun.

Group III.a: below the main-sequence

- EC14026 stars — periods: 1.5–8 minutes
  — These are pulsating hot sub-dwarf B (sdB) stars, on the 'horizontal branch' of the H-R diagram, which are multi-periodic. They form a new class, and to date about 12 stars have been confirmed as members. One EC14026 star has been observed to have an amplitude of about 0.3 mag with a period of 8 minutes, but most have

[6] In the GCVS, classified under *rotating variable stars*: "ACVO – Rapidly oscillating α^2 CVn variables".

amplitudes of around 0.02 mag with periods less than 3 minutes. These stars were theoretically predicted to be p-mode pulsators (Fontaine et al. 1998).

Group III.b: below the main-sequence, non-radial g-modes

- Planetary nebula nuclei variables (PNNV) — periods: 10–35 minutes
  — PNNV are pre-white-dwarf stars situated in the centre of planetary nebula, which are multi-periodic pulsators. They have been observed to pulsate with amplitudes of around 0.1 mag.
- DO-type variables (DOV), PG 1159 stars, GW Vir stars — periods: 5–15 minutes
  — DOV are pulsating pre-white-dwarf stars, similar to the PNNV, but without a surrounding nebula. The DOV and PNNV are located in the 'GW Vir instability strip', and many have temperatures greater than 100 000 K.
- DB-type variables (DBV) — periods: 2–18 minutes
  — DBV are multi-periodic pulsating white-dwarfs with Helium atmospheres and temperatures of around 22 000 K.
- DA-type variables (DAV), ZZ Ceti stars — periods: 1.5–20 minutes
  — DAV are multi-periodic pulsating white-dwarfs with Hydrogen atmospheres and temperatures of around 12 000 K.

Cepheids, RR Lyrae, δ Scuti and roAp stars are located in the instability strip (parallel dashed-lines). Additionally, the DAV white-dwarfs can be regarded as being located where an extension of the instability strip crosses the white-dwarf evolution track (dotted line). This suggests that these classes of stars have a similar pulsation mechanism (e.g, Cox 1980, Unno et al. 1989). For the well-studied Cepheids, this mechanism is related to the ionization zones of Hydrogen and Helium.

For a star to be unstable to pulsation in a particular mode (self-excited), there must be a driving force applied at the appropriate moment during the pulsation in order to overcome damping mechanisms. A simple analogy is a person pushing a swing: a push must be applied just after the swing reaches its highest point, for maximum effect. With an ionization mechanism, regions in the midstages of ionization of an abundant element are absorbing heat when they are most compressed. Therefore, maximum pressure in the relevant regions occurs after maximum compression and pulsations can be driven. For a Cepheid, these regions are in the outer stellar layers where the pulsation amplitude is high and the driving can outweigh the damping from the inner regions where the amplitude is low. However, we would normally expect damping from above the ionization zone to cancel the driving. In Cepheids, this is not the case because the ionization zone straddles the transition region between the quasi-adiabatic interior and non-adiabatic exterior, and the damping is reduced in the non-adiabatic exterior (see Cox 1980 for details). It is because of this condition, that the instability strip covers a narrow range of temperatures in the H-R diagram.

For the roAp stars, the pulsation mechanism is not well-known. It may be related to the He^+ ionization zone, but this is currently a matter of debate and ongoing research (e.g., Dziembowski & Goode 1996, Gautschy et al. 1998).

Chapter 2

Time-series spectroscopy

2.1 Introduction

Observational study of pulsating stars usually involves measuring variations in quantities, called 'observables', derived from the light emitted from a star. Such measurements are made using time-series spectroscopy, photometry or interferometry (a relatively new possibility). A time series can range from taking an exposure every ten seconds for an hour, in the case of photometry of a rapid oscillator, to one measurement every few months for several years, in the case of studying long-period variables.

Depending on the observable, the measured variation can be related to variations in one or more of the properties of the star: luminosity, radius, temperature, velocity ($v = \mathrm{d}R/\mathrm{d}t$ for radial pulsation), etc.; see Table 2.1 for examples. In general, these properties are not uniquely defined and will depend on the spectral region or line being measured. This is because the light from a star is emitted from a range of depths in its atmosphere. Additionally, in the case of non-radial pulsation, the variation of these properties will be a function of position on the surface.

For spectroscopy using a narrow slit ($\lesssim 2$ arcsec wide), absolute intensity measure-

Table 2.1 Observables for pulsating stars

observable	technique	properties
magnitude	photometry[a]	L, T
angular diameter	interferometry[b]	R
Doppler shift	spectroscopy	v
equivalent width	spectroscopy	T
line profile	spectroscopy	T, v

[a] Usually using Johnson or Strömgren filters.
[b] It is only recently becoming possible to measure directly radius changes of pulsating stars (Cepheids and Miras).

ments can not be made, because the total light entering the spectrograph will vary significantly between exposures as the projection of a star on the slit moves. Therefore, this type of spectroscopy is generally used to study absorption and emission lines in a star.

The most easily interpretable measurement is the Doppler shift of a line. Ignoring relativistic effects, the observed shift is an integral of the projected line-of-sight velocities across and through the observable atmosphere of a star. Therefore, the pulsational velocity of the surface away from the centre is usually larger than the measured pulsational Doppler shift[1] by a 'projection factor', which is about 1.4 for the radial pulsations in Cepheids (Albrow & Cottrell 1994). For non-radial pulsations, the situation is more complicated, the projection factor depends on the mode and the angle between the pulsation pole and the line of sight.

The equivalent-width (EW) of a line is a measure of the strength of absorption or emission relative to the continuum (the EW is positive for absorption, and negative for emission). If a spectrum (intensity versus wavelength) is normalised so that the continuum emission has an intensity of 1, then the EW is defined as $(1 - I) \times W$ where I is the mean intensity across a spectral region of width W that includes the line only. Changes in the EW of a line during pulsation are mainly related to temperature changes at the formation depth of the line, but can also depend on pressure and density changes.

A spectral line may change in a complicated way that can not easily be quantified by two parameters (Doppler shift and EW), for instance: (i) a line may be asymmetrical, in which case, the value of the Doppler shift will depend on how it is measured; or (ii) there may be emission and absorption components to a spectral line. In these cases and others, it becomes relevant to investigate changes in the line profile as a whole. Line profile changes can be quantified using bisector or intensity measurements, i.e., resolving the line vertically or horizontally. Alternatively, they can be qualitatively studied by plotting the line profile as a function of pulsation phase.

2.2 Observing

There are many techniques for observing pulsating stars using spectroscopy depending on the pulsation period, brightness, what properties are being studied, etc. To determine a suitable method, it is necessary to consider the science requirements in terms of: resolution; signal-to-noise; wavelength range; instrument stability; frequency and number of observations. In this section, the observations of the three stars analysed in this thesis are explained.

Most of the observations were taken using the coudé spectrograph[2] on the 74-inch (188-cm) Telescope at Mt. Stromlo. A Schmidt camera, with a focal length of 32 inch

[1] To obtain the pulsational Doppler shift, the centre-of-mass velocity and other non-pulsational line shifts must be removed from the measurements. Other line shifts can be caused, for example, by convection where the integral of the velocities is weighted towards rising gas in the convective regions and the observed line will appear blue-shifted, even though there may be no net-motion of the surface.

[2] The light enters the spectrograph through a slit mounted at the coudé focus (situated below the telescope). The light is then collimated, dispersed and refocused onto a detector.

(81 cm), focuses the spectrum onto a Tektronix CCD, which was about 5 x 5 cm in size with 2000 x 2000 pixels.

Mt. Stromlo is a good site for studying bright pulsating stars because it is a poor site! To explain this comment — it is a poor site in terms of light pollution (from Canberra), seeing and weather, which means that it is less subscribed by astronomers studying faint objects or by those needing good seeing or photometric conditions. Therefore, more time is available for astronomers doing spectroscopy of bright stars. This is good for studying pulsations because large blocks of time can be obtained for observing projects (two or more weeks), which is important: (a) for good frequency-resolution in the oscillation spectrum of rapidly oscillating stars, or (b) for good phase-coverage of pulsations in Cepheids. In other words, the length of observing time is of high importance and, while good conditions will obviously improve results, observing conditions are less critical than in other areas of astronomy. Also, at low altitude sites such as Mt. Stromlo, absorption lines from the Earth's atmosphere are stronger and more stable. This can actually be an advantage if these telluric lines are being used as a velocity reference (see Section 5.5.1).

For the study of the Hα line in ℓ Car (Chapter 4), the observations[3] were part of a project to determine accurately the radial velocity curves of a few Cepheids, e.g., ℓ Car (Taylor et al. 1997) and β Dor (Taylor & Booth 1998). Several sets of observations were made in 1994 and 1995 (see Table 4.1) with good phase coverage of the pulsation in ℓ Car ($P = 35.5$ d), the largest gap being 0.085 of a cycle (3 days). The main project requirements were high resolution and a large wavelength range that included Hα, Hβ and many metal lines for accurate velocity analysis. For this purpose, the echelle setup was used. The light was first dispersed by a cross disperser grating (158 grooves/mm) and then by the echelle grating (31.6 grooves/mm). About 45 orders (different wavelength regions) were projected on to the CCD, with a total wavelength coverage from about 4800Å to 6800Å. The dispersion was about 2.2Å/mm (0.05Å/pixel) at 6000Å with a resolution of about 2 pixels (0.1Å). To calibrate the wavelength range for each order and to remove instrumental shifts, several Thorium-Argon arc spectra were taken during each observing night.

For α Cir (Chapters 5–6), the observations were part of a dual-site campaign[4] (at Stromlo and La Silla) to study this star and a δ Scuti star FG Virginis. The Stromlo observations covered two weeks in May 1996, with observing concentrated on α Cir in the second week (see Table 5.1). The main requirements were high frequency of exposures, high signal-to-noise and a wavelength range that included Hα and the telluric lines around 6900Å (to be used as a velocity fiducial). For this purpose, the light was dispersed using a single reflection grating, the B-grating, which had 600 grooves/mm. The grating was used to project 1st-order spectra on to the CCD, giving a dispersion of 20 Å/mm (0.49Å/pixel). A slit width of about 0.5 mm was used, giving a resolution of about 3 pixels (1.5Å). The total wavelength coverage was from 6000Å to 7000Å.

The observing of a single order spectrum allowed a small part of the CCD to be read-

[3]The observations were done mainly by Melinda Taylor.

[4]Multi-site campaigns are often organised to study pulsating stars ($P \lesssim 1$ day), because this reduces 1/day aliases in the oscillation spectrum.

out, a window of 2000 x 40. This produced a fast read-out time of 17 seconds which was important in obtaining a high frequency of exposures. Due to the way the CCD reads out data, a window of 40 x 2000 had a significantly longer read-out time (about 55 seconds), therefore, at the start of this observing run the CCD was rotated by 90 degrees from its usual position. This rotation allowed almost twice as many exposures to be taken (one per 45 s compared to one per 83 s), because the exposures of α Cir were limited to 28 seconds (on average) to avoid saturating the CCD.

For HR 3831 (Chapter 7), a similar setup to α Cir was used, essentially to apply the same techniques to a different roAp star. The differences were: (a) a slightly higher wavelength coverage, 6100-7100Å; and (b) a wider CCD window, 2000 x 80, to improve scattered light subtraction, with the read-out time only increased by 3 s to 20 s. The exposure time was chosen to be 100 seconds, using the calculation described below.

2.2.1 Calculation of optimum integration time

In this section, I look at the optimum strategy for observing a pulsating star in terms of the integration time per exposure. In particular, I am considering the case where the expected pulsations are rapid enough that phase smearing becomes an issue. Phase smearing is the reduction in the measured amplitude due to the effect of integrating over a significant fraction of a pulsation cycle. This will typically be an issue for pulsation periods of less than an hour or so.

The aim is to maximise the signal-to-noise ratio in the amplitude spectrum of a time series covering a given total observing time (A typical amplitude spectrum is shown in Figure 5.4). The two factors that I am considering are:

(i) fraction of time spent integrating light from the star (duty-cycle),

(ii) reduction in amplitude of a sine-wave due to integration (phase smearing).

The principal assumption, in this calculation, is that the final noise level will be proportional to $\sqrt{1/D}$, where D is the duty-cycle. For instance, this will be the case for measurements that are dominated by photon noise.

The important variables are:

- I — integration time per exposure,
- P — period of oscillation,
- R — read-out time or over-head time between exposures.

The duty-cycle can be written as

$$D = \frac{I}{I+R} \,. \tag{2.1}$$

Consider a sine wave of frequency $\omega = 2\pi/P$ and amplitude A . We wish to determine how the measured amplitude (A_m) is reduced with integration time. $V_m(t)$ is the measured observable at a time t (mid-time of the exposure):

$$V_m(t) = \frac{1}{I}\int_{t-I/2}^{t+I/2} A\,\sin(\omega t')\,\mathrm{d}t' = \frac{A}{\omega I}[\,\cos(\omega(t-\frac{I}{2})) - \cos(\omega(t+\frac{I}{2}))\,] \,. \tag{2.2}$$

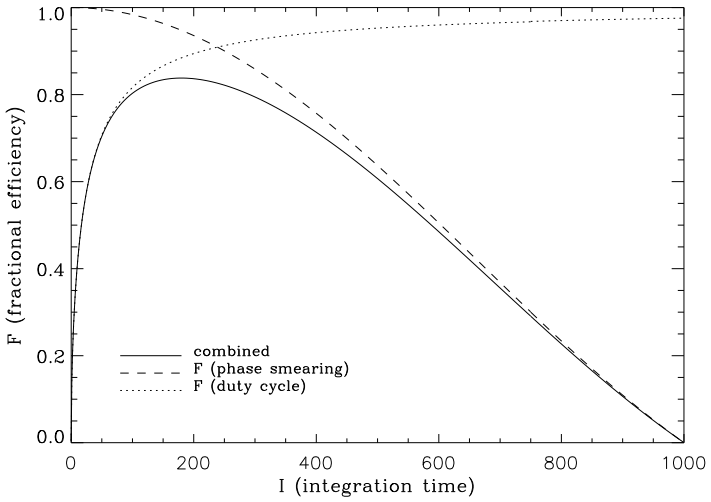

Figure 2.1 Efficiency of observing a star with a pulsation period of $P = 1000$ seconds and an over-head time between exposures of $R = 50$ seconds. The effects of phase smearing and duty cycle are shown separately and combined.

Using cosine identities, this can be simplified to

$$V_m(t) = \frac{2A}{\omega I} \sin\left(\frac{\omega I}{2}\right) \sin(\omega t) \,. \tag{2.3}$$

Setting $V_m = A_m \sin(\omega t)$, we have

$$A_m = \frac{\sin(x)}{x} A \,, \quad \text{where} \quad x = \frac{\omega I}{2} = \frac{\pi I}{P} \,. \tag{2.4}$$

This quantifies the effect of phase smearing. At the limit $I \to 0$ then $A_m = A$; and if $I = P$ then $A_m = 0$. The signal-to-noise ratio is proportional to $\sqrt{D} \times (A_m/A)$, which is the fraction F of the most efficient observing ($F = 1$ in the theoretical limit of $R = 0$ and $I \to 0$).

$$F = \sqrt{D}\frac{A_m}{A} = \sqrt{\frac{I}{I+R}} \frac{\sin(\pi I/P)}{(\pi I/P)} = \frac{P}{\pi\sqrt{I(I+R)}} \sin\left(\frac{\pi I}{P}\right) \,. \tag{2.5}$$

An example of F as a function of I is shown in Fig. 2.1 for a pulsation period of 1000 seconds with an over-head time between exposures of 50 seconds. The figure shows the effect of the two factors separately and combined. The combined curve is fairly flat at the top and integration times ranging from 100 to 250 seconds would give an F-value of greater than 0.8. Therefore there is plenty of room to vary I in consideration of other factors, while maintaining a good F-value in terms of this analysis. For instance, there may be other pulsation periods within the same star to consider. Fig. 2.2 shows the effect of changing the pulsation period on the F versus I curve, with R constant (20 seconds).

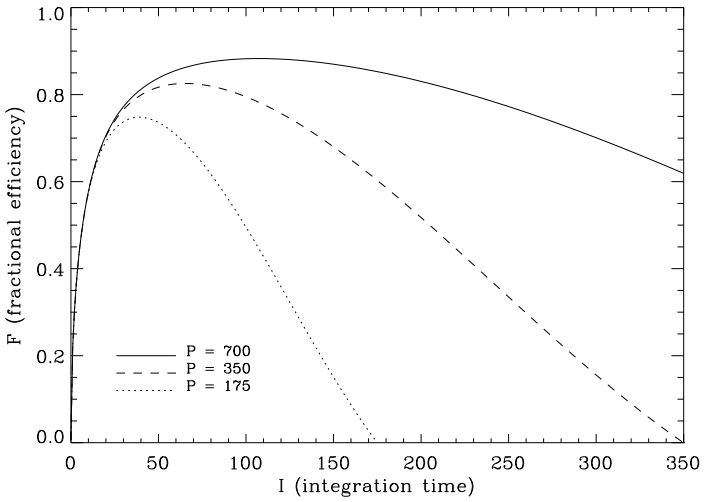

Figure 2.2 Efficiency of observing a star with several pulsation periods and an over-head time of $R = 20$ seconds. These periods are equal to the principal, 1st harmonic and 3rd harmonic pulsation periods in HR 3831.

I used this analysis to determine the optimum integration time for the observing run on HR 3831 during March 1997 (Section 7.2.1). I chose to use an integration time of 100 seconds which was close to the optimum time for detecting the principal frequency and which also gave a reasonable F-value for the first harmonic. Higher order harmonics were not considered, since I was mainly interested in determining the properties of the principal frequency.

For the observations of α Cir during May 1996 at Mt. Stromlo (Section 5.2), with the principal oscillation period of 410 seconds and an over-head time of 17 seconds, the optimum integration time was calculated to be 70 seconds. However, during this observing run, the integration time was limited by the digital saturation of the CCD. I varied the integration time between 20 and 45 seconds depending on the conditions (seeing and extinction), with the aim of maximising the duty-cycle without saturating any images.

In summary: for observations of a singly periodic star where the final noise level in the amplitude spectrum is expected to be approximately proportional to $\sqrt{1/D}$, the integration time should be chosen to maximise F according to Equation 2.5. If several pulsation periods *of equal interest* are being studied in a star, the F-value should be chosen for the shortest period because, in any case, it will be higher for longer periods. In consideration of other noise factors: if there is a noise level in the final analysis that is independent of the duty cycle, higher weight should be given to the effect of phase smearing and therefore the integration time should be lower. Conversely, if read-out noise is a significant factor, increasing the duty-cycle is more important and therefore the integration time should be higher.

Note that the above analysis was made by considering a fixed total observing time. The signal-to-noise ratio in the final amplitude spectrum can be increased by observing

for longer, as long as an oscillation remains coherent, i.e., with no significant phase jumps or frequency changes. The noise level in the amplitude spectrum will be, approximately, inversely proportional to the square-root of the total observing time.

2.3 Data reduction

CCDs consist of an array of pixels (typically 2000 x 2000 pixels). During an exposure, incident photons are stored as electrons in each pixel. After the exposure is finished, the CCD is read out, which means the charge in each pixel is converted to a digital number called analogue-to-digital units (ADU; usually a 16-bit integer 0–65535). In addition to the science spectral images, several calibration images are usually taken — these include: biases, flat-fields, dark images, arcs and standard stellar spectra. The initial reduction process involves converting the 2D science spectral images to 1D spectra (relative intensity vs. wavelength), using the calibration images to improve accuracy. The methods, as applied to the data analysed for this thesis, are briefly outlined in the results chapters (4–7). In this section, I describe in more detail some of these methods as a general guide [(i)–(vii) below].

The main software packages used were FIGARO, developed by Keith Shortridge, and IRAF, maintained by the National Optical Astronomy Observatories (NOAO). These packages have similar capabilities for analysing astronomical data.

(i) Bias subtraction — Every CCD digital image has a zero-point offset to the measured number of photons, which is called the bias (typically around 1000 ADU). The bias level can vary over the CCD (bias structure) and can vary from image to image. The reduction generally involves two stages: (a) subtraction of a bias frame, which is obtained by reading out the CCD without exposing it to light; and (b) adjustment to the zero level using over-scan regions of the image, which are regions that are not exposed to light during an exposure on the rest of the CCD. As with all images, the bias images will contain read-out noise. To avoid introducing unnecessary extra noise into the images of the spectra, ten or more bias images can be averaged to produce a low noise-level bias frame.

(ii) Non-linearity correction — For a linear CCD, the measured ADU counts (after bias subtraction) will be proportional to the number of incident photons. However, no CCD is perfectly linear, and in some cases, the accuracy of results can be significantly improved by making a non-linearity correction. This is the subject of Chapter 3.

(iii) Flat-field correction — The quantum efficiency, or probability of capturing photons, can vary from pixel to pixel on a CCD (typically by a few percent). This can be corrected by dividing the images of the spectra by a flat-field frame, which is made by processing images of the spectrum of a bright lamp that has no spectral-line features. The processing can involve bias subtraction, non-linearity correction, averaging and illumination correction.

Figure 2.3 A CCD image of an echelle spectrum

Any pixel-to-pixel variations in a flat-field image are due to intrinsic variations of the CCD, noise or illumination. The noise can be reduced by averaging many flat-field images, so that the percentage noise variations are significantly smaller than the percentage intrinsic variations. If the illumination of the lamp on the CCD is significantly different from the star light (along the dispersion direction), it may be necessary to remove illumination variation of the flat-field. This can be done by dividing by a smoothed version of the flat-field, in effect, leaving only the high-frequency intrinsic variations.

(iv) Cosmic ray removal — When a high-energy particle interacts with a CCD, a number of extra electrons are left in one or a few neighbouring pixels. These can be removed by comparing similar images, or by searching for and interpolating over spikes in an image. The easiest method, for biases and flat-fields in particular, is to take the median value (pixel by pixel) of three or more images. For spectral images, obvious spikes can be removed before or after extracting the spectra. With thousands of short exposures, as with the observations of α Cir and HR 3831, it is unnecessary to remove cosmic rays because each measurement has very little chance of being contaminated and bad data-points can be removed when the time-series analysis is applied.

(v) Tracing and extraction of spectrum — Spectra are projected onto two-dimensional images (Figure 2.3). One dimension represents the dispersion direction and the other represents the slit direction (the spread of light along the slit due to seeing or tracking). In the case of an echelle spectrum, several wavelength regions (called orders) are projected onto different parts of the CCD, the dispersion direction remains nearly the same and the different orders are separated from each other in the slit direction so that light from adjacent orders does not overlap. In reality, the dispersion direction is never exactly horizontal or vertical, and therefore, the first part of this

reduction is to trace the peak of the spread of star light (in the slit direction), along the dispersion axis. This must be done for each order, with typically a quadratic fit to the trace. The second part is to extract the order(s), by adding-up the counts in the slit direction within typically ten pixels of the centre of the trace at each point along the dispersion axis.

As well as star light dispersed onto the CCD, there will be scattered star light and background sky light. This extra light can be removed by measuring the light intensity on either side of the extracted spectrum (in-between the orders of an echelle spectrum), and then subtracting an appropriately scaled value. For example, 10 lines are added-up to determine the extracted spectrum and 20 lines to determine the scattered light, then 0.5 times the scattered light is subtracted from the spectrum. This process 'adds' photon and read-out noise to a spectrum but it is necessary if accurate relative intensity measurements are to be made, because the ratio between the scattered / background light intensity and the true spectral intensity can vary from exposure to exposure.

(vi) Continuum fitting — It is generally not possible to make absolute intensity measurements in medium- to high-resolution spectra because slit losses vary. Therefore, the continuum emission is usually taken as a reference level. The intensity and shape of this continuum level can vary from exposure to exposure. To overcome this, a fit can be made to continuum or near-continuum regions in order to normalise the continuum level to an intensity of 1.0 across the spectrum. Continuum fits with only a few parameters are more robust, while those with more parameters are potentially more accurate. When reducing thousands of spectra, as in the case of α Cir and HR 3831, robustness is important and typically a 2nd or 3rd degree polynomial is used. For a few spectra, the continuum fit can be checked and adjusted by eye and any type of fit can be tried to obtain high accuracy. In the case of spectra with many absorption lines, sometimes only a poor approximation can be made to the continuum level.

In the case of echelle orders, the shape of the continuum is noticeably curved due to the grating diffraction pattern. Therefore, it may better to correct for this illumination shape before applying a continuum fit. This can be done by dividing by a smoothed flat-field order or by a good fit to an order of a stellar spectrum which has few lines (for example, the spectrum of an early-type-B star).

(vii) Wavelength calibration — The orders, once extracted, will be in the form of intensity versus pixel-number. In order to calibrate the pixel-number in terms of wavelength, it is useful to take spectra of an arc lamp (e.g., a Th-Ar arc). The positions of the emission lines with known wavelengths are then identified, and a fit is made to the dispersion across the order. Typically, a quadratic fit is adequate.

For ℓ Car (Chapter 4), further reduction involved converting the wavelengths to heliocentric values and determining the pulsational phase for each observed spectrum.

For α Cir and HR 3831, more than a thousand spectra were observed in each case, and the changes from one spectrum to the next were too small to interpret by eye. Further

reduction consisted of measuring observables from each spectrum, and determining their oscillation amplitudes and phases through time-series analysis. These processes are described in detail in the results chapters (e.g., in Sections 5.3, 6.2, 7.3). For this specialised analysis, I wrote or modified programs in the commercial package IDL or in FORTRAN.